ACS APPLIED MATERIALS & INTERFACES

RESEARCH ARTICLE

www.acsami.org

Facile Fabrication and Thermoelectric Properties of PbTe-Modified Poly(3,4-ethylenedioxythiophene) Nanotubes

Yuanyuan Wang, Kefeng Cai,* and Xi Yao

Tongji University, Functional Materials Research Laboratory, 1239 Siping Road, Shanghai 200092, China

Supporting Information

ABSTRACT: In this paper, we presented a facile route to poly(3,4-ethylenedioxythiophene) (PEDOT) and PbTe-modified PEDOT nanotubes. The nanotubes were prepared by an in situ interfacial polymerization method. The phase structure and morphology of the powders were characterized by X-ray powder diffraction, infrared spectroscopy, and transmission electron microscopy, respectively. The thermoelectric properties of the powders after being cold pressed were measured at room temperature. The materials exhibit extremely large Seebeck coefficient values, which is promising for thermoelectric applications.

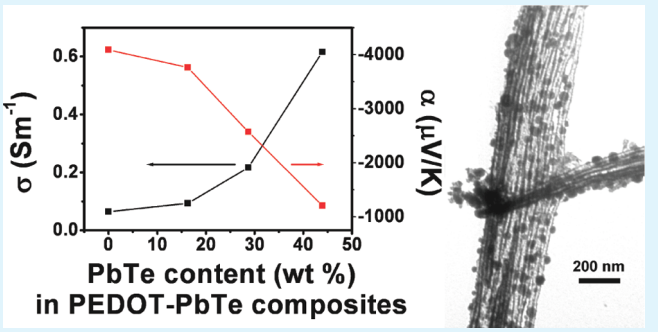

KEYWORDS: poly(3,4-ethylenedioxythiophene), PbTe, nanotubes, interfacial polymerization, thermoelectric

1. INTRODUCTION

Thermoelectric (TE) materials have recently attracted much attention for their potential applications in harvesting electricity from waste heat, cooling, and thermal sensing. The effectiveness of a TE material is determined by its dimensionless figure of merit, $ZT = \alpha^2\sigma T/\kappa$, where T is the absolute temperature, α the Seebeck coefficient, σ the electrical conductivity, and κ the thermal conductivity of the material.

Traditionally, the studies on high performance TE materials are mainly focused on inorganic semiconductors, such as Bi_2Te_3 and its alloys,[1,2] PbTe and its alloys,[3,4] filled $CoSb_3$ skutterudites,[5] and clathrates.[6] Recently, increasing attention has been paid to organic materials, especially conjugated polymers, such as polyaniline, polypyrrole, polythiophene, and their derivatives.[7−12] Conjugated polymers usually have much lower thermal conductivity than inorganic materials, which is beneficial to the enhancement of the ZT value. Moreover, compared with inorganic TE materials, the conjugated polymers are flexible and easily fabricated. One of polythiophene derivatives, poly(3,4-ethylenedioxythiophene) (PEDOT), becomes more and more important in the family of conjugated polymers because of its low redox potential, high electrical conductivity, and good environmental stability.[13] It has been applied in various fields, such as plastic electronics,[14] light-emitting diodes,[15] organic transistors,[16] antistatic coatings,[17] and sensors.[18] However, up to now, only a few studies have been conducted on TE properties of PEDOT. Jiang et al.[7] prepared PEDOT:poly(styrenesulfonate) (PSS) powder and measured the properties of the powder after being cold pressed. The compacted powder showed low thermal conductivity, moderate electrical conductivity, but very low positive Seebeck coefficient (12−16 μV/K).

Theoretical calculations and experiments have both shown that low-dimensional TE materials have enhanced ZT values due to the quantum size effect and enhanced interface scattering of phonons.[1,3,19−22] Several methods have been developed to prepare PEDOT nanostructures, such as the microemulsion[23] and reverse microemulsion[24] polymerization methods, electrochemical synthesis,[25,26] and V_2O_5 seeding approach.[27] Compared with these methods, interfacial polymerization is more facile.[28] Su et al.[29] synthesized PEDOT nanoneedles at a dichloromethane/water interface. In this work, we developed a chemical oxidative method at the interface between *n*-hexane and acetonitrile for synthesis of PEDOT nanotubes.

Compared with traditional inorganic TE materials, the ZT value of conjugated polymers is still very low. Composite materials consisting of inorganic nanostructures and polymer may have better TE properties than pure polymer, as the composite materials could inherit the properties of both the polymer and the inorganic nanostructures and even have a synergistic effect. Kim et al[30] show that an enhanced TE property could be obtained by filling carbon nanotubes into PEDOT:PSS, which has much higher electrical conductivities than pure polymer without significantly altering Seebeck coefficient. In our previous work, we studied the transport properties of PbTe-polyaniline composite nanopowders. The composite shows much higher electrical conductivity than pure undoped polyaniline and a larger Seebeck coefficient than both PbTe and polyaniline.[31] In this work, PbTe-modified PEDOT nanotubes were in situ fabricated at room temperature by an interfacial polymerization method. The TE properties of the PEDOT and the composite powders after cold pressing were measured at room temperature.

Received: December 31, 2010
Accepted: March 2, 2011
Published: March 02, 2011

2. EXPERIMENTAL PROCEDURES

The 3,4-ethylenedioxythiophene (EDOT) monomer was purchased from Suzhou Yield Pharma Co., Ltd., China, and other reagents were purchased from Sinopharm Chemical Reagent Co., Ltd., China. All reagents were analytical grade and directly used without further purification.

2.1. Interfacial Polymerization of PEDOT Nanotubes. In a typical run, 0.02 mol $FeCl_3$ was dissolved into 50 mL acetonitrile under magnetic stirring (solution A). A total of 1 mL (≈0.01 mol) of EDOT was dissolved in 30 mL *n*-hexane (solution B). Solution A was dropped into solution B at one drop every 2 s, and the mixture was kept stirring at room temperature for 24 h. The product was collected from the polymerization media by centrifugation and rinsed with deionized water and absolute ethanol in sequence more than 10 times, then separated by centrifugation for 5 min at 4000 rpm and finally dried in vacuum at 70 °C. During the washing procedure, the color of the product changed from dark green to black, indicating that the virgin doped product was dedoped and became a reduced state. The final black product is called sample I.

2.2. In Situ Fabrication of PbTe-Modified PEDOT Nanotubes. PbTe nanoparticles (about 50 nm in diameter) were synthesized by a chemical bath method at room temperature as described in ref 32.

A typical procedure for fabrication of the PEDOT-PbTe composite is as follows: 50 mL solution A and 30 mL solution B were first prepared. A total of 0.25 g of the PbTe nanoparticles were added into solution B and then ultrasonically dispersed for 1 h. Solution A was dropped into the PbTe dispersed solution at one drop every 2 s, with consistently magnetic stirring. About 24 h later, the mixture was centrifuged, and the precipitates were washed with deionized water and absolute ethanol in sequence many times. Finally, the product was dried in vacuum at 70 °C. The product is called sample II. The PbTe content (c) was calculated by the equation: $c = w_1/w \times 100\%$, where w_1 is the weight of PbTe nanoparticles added into the reaction system, and w is the weight of the final product. The PbTe content of sample II was estimated to be 16.3 wt %.

The procedure was repeated by adding 0.5 and 1.0 g PbTe nanoparticles, and the content of PbTe in the corresponding composite powder was estimated to be 28.7 and 43.9 wt %, respectively.

2.3. Characterization. The samples were examined by X-ray diffraction (XRD) performed on a Bruker D8 Advanced X-ray Diffractometer with Cu K_α radiation (λ = 1.5406 Å). The morphology of the samples was observed by transmission electron microscopy (TEM, Hitachi H-800). FT-IR spectrum of each sample was obtained with an Equinox SS/Hyperion 2000 FT-IR spectrometer.

The powder samples were cold pressed into pellets (10 mm in diameter and about 1 mm in thickness) at ~10 MPa for the electrical conductivity and Seebeck coefficient measurement. The bulk electrical conductivity of each pellet was measured by a two-probe method: the pellet was sandwiched with two round-disk copper electrodes. The Seebeck coefficient was determined by the slope of the linear relationship between the thermal electromotive force and temperature difference (~10−16 K) between the two sides of each pellet (see Supporting Information). The error of the measured Seebeck coefficient values is <10%.

3. RESULTS AND DISCUSSION

Figure 1 shows the infrared spectra of the samples I and II. The spectrum (a) in Figure 1 corresponds to that for PEDOT. The peaks at 682, 839, and 981 cm^{-1} are related to C−S bond stretching vibration in thiophene rings, and the absorption peaks at 1512 and 1344 cm^{-1} are assigned to the C−C or C═C stretching vibration of thiophene rings. The peaks at 1054, 1089, and 1203 cm^{-1} could be attributed to the stretching of C−O−C

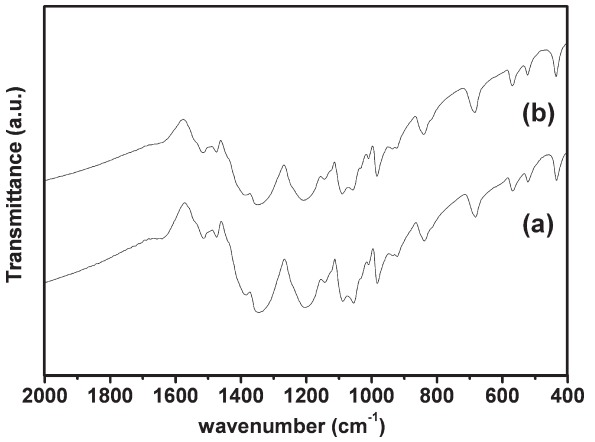

Figure 1. FT-IR spectra of (a) sample I and (b) sample II.

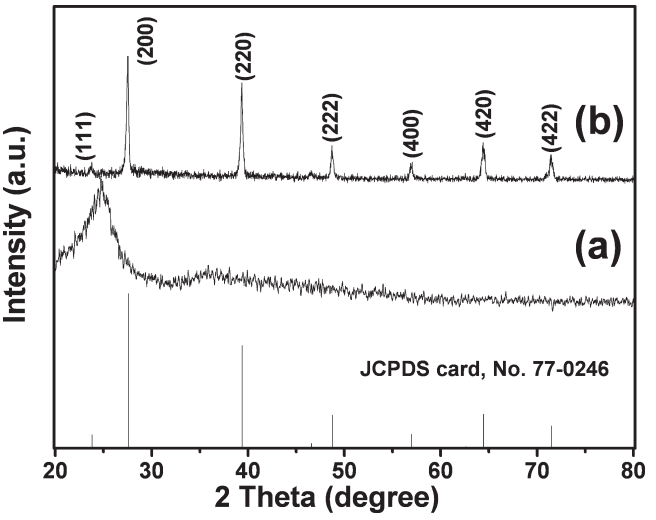

Figure 2. Typical XRD patterns of (a) sample I and (b) sample II. The standard XRD pattern of PbTe alloy (JCPDS card file, No. 77-0246) is also given for comparison.

bonds. The absorption peak at about 1640 cm^{-1} is very weak and broad, indicating that the PEDOT is basically dedoped after the purification procedure.[13,33] Spectrum (b) is very similar to spectrum (a), indicating that sample II contains PEDOT. There is no obvious peak for PbTe in spectrum (b) because of the much weaker vibrational energy absorption of PbTe than that of PEDOT within the infrared region.

Figure 2 shows typical XRD patterns of samples I and II. The pattern of sample I (Figure 2(a)) is a typical amorphous pattern with a low and broad peak at about 24.8°, indicating that the PEDOT is not well crystallized. The pattern of sample II (Figure 2(b)) can be indexed to the reported PbTe (JCPDS card file, No. 77-0246). The peak at 24.8° for PEDOT in Figure 2(b) is not obvious because of its much weaker diffraction intensity. Combining the FT-IR and XRD results, it can be deduced that sample II consists of PbTe and PEDOT.

A typical TEM image of sample I is shown in panel (a) of Figure 3 . It is shown in panel (a) of Figure 3 that sample I mainly consists of PEDOT nanotubes, which tend to combine together side-by-side. The diameter of the PEDOT nanotubes is about 50 nm, and the length of the nanotubes ranges from 0.5 to 1.5 μm.

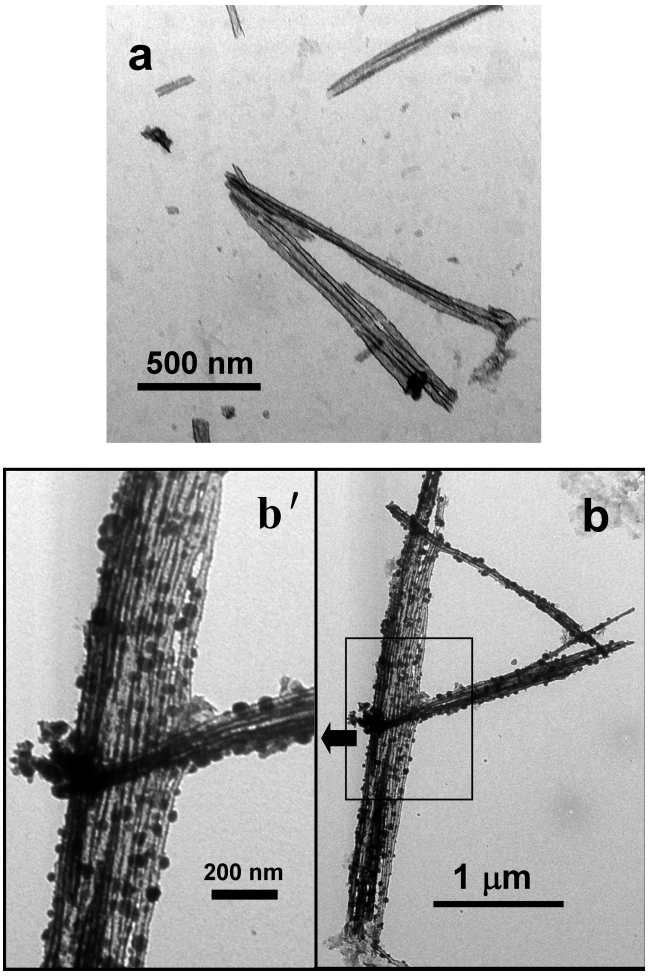

Figure 3. Typical TEM images for (a) sample I, (b) sample II, and (b′) high magnification image of the marked zone in (b).

Panel (b) of Figure 3 is a typical TEM image for sample II at low magnification. It is shown in panel (b) of Figure.3 that sample II consists of PEDOT nanotube clusters coated with PbTe nanoparticles (~20−50 nm), which can be more clearly seen from the high magnification image (Figure 3(b′)). The length of the PEDOT nanotubes is more than 4 μm. Panel (b′) of Figure 3 shows that the diameter of the PEDOT nanotubes is about 40 nm.

On the basis of the above results, the formation mechanism of the composite nanostructures is suggested as follows: during the synthesis procedure of the pure PEDOT, $FeCl_3$ was dissolved in acetonitrile, while EDOT dissolved in *n*-hexane. At the acetonitrile/*n*-hexane interface, EDOT was oxidatively polymerized by Fe^{3+}, and the newly formed PEDOT nanotubes entered into the acetonitrile phase. When the PbTe nanoparticles were added into the reaction system, they were situated at the acetonitrile/*n*-hexane interface and absorbed on the surface of the PEDOT nanotubes. Moreover, the PbTe nanoparticles could be a solid-stabilizer and assist to form a solid-stabilized emulsion (often called Pickering emulsion[34]), which has much finer droplets of the mixture than that made by simply agitation. As a result, the PEDOT nanotubes of sample II are longer and thinner than those of sample I.

The room-temperature electrical conductivity, Seebeck coefficient, and power factor of the powders after cold pressing as a function of PbTe content are shown in Figure 4. Panel (a) of Figure.4 shows that the electrical conductivity of the pure PEDOT is very low (0.064 $S \cdot m^{-1}$). This is because the PEDOT is dedoped, which leads to a very low carrier concentration. When the PbTe content increases to 43.9 wt %, the electrical conductivity of the sample increases to 0.616 $S \cdot m^{-1}$ due to the PbTe with higher electrical conductivity. However, the value is still much lower than that of cold-pressed PbTe nanoparticles (8.2 S m^{-1}),[31] indicating that the PbTe nanoparticle content is not high enough to form a percolation network. It is shown in panel (a) of Figure 4 that all the samples have negative Seebeck coefficients (which is not as we expected), and the absolute Seebeck coefficient value decreases with increasing PbTe content. The doped PEDOT usually shows P-type conduction because the charge carrier is a positive polaron or bipolaron created by counterions. In this work, the counterions (Cl^-) were removed during the purification procedure, and the PEDOT changed from an oxidized state to a neutral one, which not only leads to a distinct decrease of carrier concentration (and thus low electrical conductivity), but also changes the type of charge carriers. The negative Seebeck coefficients may be attributed to the conjugated electrons in the neutral PEDOT chains. Sample I has an extremely large absolute Seebeck coefficient value (4088 $\mu V\ K^{-1}$), which is about 20 times as large as that of state-of-the-art TE materials, such as Bi_2Te_3, at room temperature. The delocalized π−conjugated structure of PEDOT with low carrier concentration usually contributes to large carrier mobility and thus a high Seebeck coefficient value. As the PbTe content is

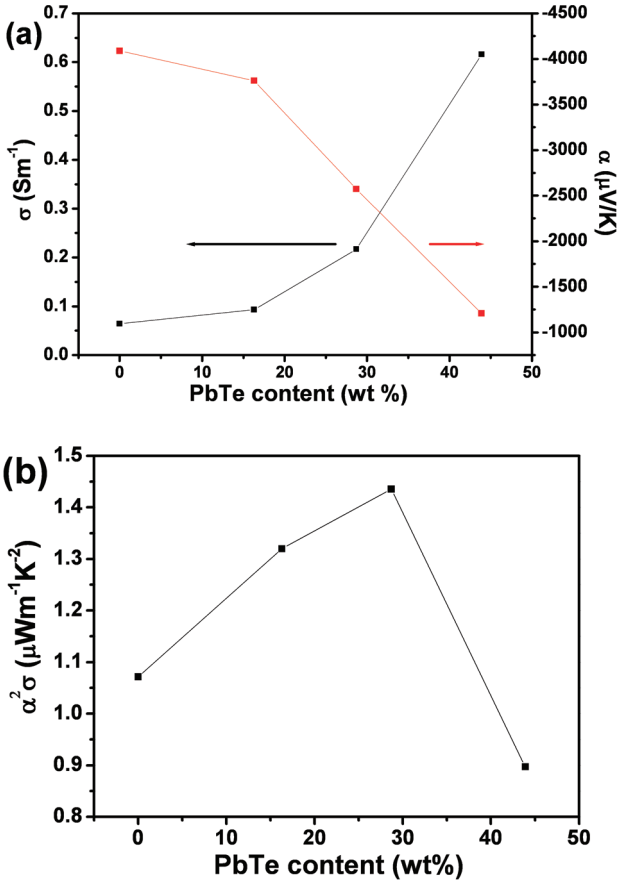

Figure 4. (a) Electrical conductivity, Seebeck coefficient, and (b) power factor ($\alpha^2\sigma$) for the composite pellets with different PbTe content.

increased, the absolute Seebeck coefficient value decreases from 4088 μV K^{-1} (pure PEDOT) to 1205 μV K^{-1} (the sample with 43.9 wt % PbTe). This is because the PbTe nanoparticles have relatively low positive Seebeck coefficients (465 μV K^{-1}).[31] Panel (b) of Figure 4 shows that the calculated power factor first increases from 1.07 μWm^{-1} K^{-2} (pure PEDOT) to 1.44 μWm^{-1} K^{-2} (28.7 wt % PbTe sample) and then decreases to 0.897 μWm^{-1} K^{-2} (43.9 wt % PbTe sample), indicating that the TE property could be tuned by adjusting the PbTe content in the composite.

As shown in panels (b) and (b′) of Figure 3, the PbTe nanoparticles are spherical, and large amounts are needed for the nanoparticles to form percolation networks. If the PbTe nanoparticles are in a one-dimensional structure, the amount of them needed to form percolation networks will be much less, and their negative effect on the Seebeck coefficient will be much less. Moreover, if the TE nanostructures used are n-type and have high electrical conductivity, the result should be better.

4. CONCLUSIONS

In summary, we developed a facile route to PEDOT nanotubes by an interfacial polymerization method. The pure dedoped PEDOT exhibited n-type conduction and had an extremely large Seebeck coefficient value (−4088 μV K^{-1}), but low electrical conductivity (0.064 S m^{-1}). PbTe-modified PEDOT nanotubes were in situ fabricated by adding PbTe nanoparticles into a polymerization media. The electrical conductivity of the composite powders after cold pressing increases with increasing PbTe content, and the power factor of the composite powders could be tuned by adjusting the PbTe content.

■ ASSOCIATED CONTENT

Supporting Information. Scheme of apparatus for measuring the thermoelectric coefficient and plot of thermoelectromotive force versus temperature difference from two sides of each sample. This information is available free of charge via the Internet at http://pubs.acs.org/.

■ AUTHOR INFORMATION

Corresponding Author
*E-mail: kfcai@tongji.edu.cn. Tel./Fax.: +86-21-65980255.

■ ACKNOWLEDGMENT

This work was supported by the National Natural Science Foundation of China (50872095) and the 973 Project under Grant 2007CB607500.

■ REFERENCES

(1) Venkatasubramanian, R.; Siivola, E.; Colpitts, T.; O'Quinn, B. *Nature* **2001**, *413*, 597.
(2) Yan, X. A.; Poudel, B.; Ma, Y.; Liu, W. S.; Joshi, G.; Wang, H.; Lan, Y. C.; Wang, D. Z.; Chen, G.; Ren, Z. F. *Nano Lett.* **2010**, *10*, 3373.
(3) Harman, T. C.; Taylor, P. J.; Walsh, M. P.; LaForge, B. E. *Science* **2002**, *297*, 2229.
(4) Hsu, K. F.; Loo, S.; Guo, F.; Chen, W.; Dyck, J. S.; Uher, C.; Hogan, T.; Polychroniadis, E. K.; Kanatzidis, M. G. *Science* **2004**, *303*, 818.
(5) Sales, B. C.; Mandrus, D.; Williams, R. K. *Science* **1996**, *272*, 1325.
(6) Nolas, G. S.; Cohn, J. L.; Slack, G. A.; Schujman, S. B. *Appl. Phys. Lett.* **1998**, *73*, 178.
(7) Jiang, F. X.; Xu, J. K.; Lu, B. Y.; Xie, Y.; Huang, R. J.; Li, L. F. *Chin. Phys. Lett.* **2008**, *25*, 2202.
(8) Kaiser, A. B. *Rep. Prog. Phys.* **2001**, *64*, 1.
(9) Toshima, N. *Macromol. Symp.* **2002**, *186*, 81.
(10) Li, J. J.; Tang, X. F.; Li, H.; Yan, Y. G.; Zhang, Q. J. *Synth. Met.* **2010**, *160*, 1153.
(11) Sun, J.; Yeh, M. L.; Jung, B. J.; Zhang, B.; Feser, J.; Majumdar, A.; Katz, H. E. *Macromolecules* **2010**, *43*, 2897.
(12) Feng, J.; Ellis, T. W. *Synth. Methods* **2003**, *135*, 55.
(13) Groenendaal, B. L.; Jonas, F.; Freitag, D.; Pielartzik, H.; Reynolds, J. R. *Adv. Mater.* **2000**, *12*, 481.
(14) Hohnholz, D.; Okuzaki, H.; MacDiarmid, A. G. *Adv. Funct. Mater.* **2005**, *15*, 51.
(15) Cao, Y.; Yu, G.; Zhang, C.; Menon, R.; Heeger, A. J. *Synth. Methods* **1997**, *87*, 171.
(16) Hong, K.; Yang, S. Y.; Yang, C.; Kim, S. H.; Choi, D.; Park, C. E. *Org. Electron.* **2008**, *9*, 864.
(17) Jonas, F.; Krafft, W.; Muys, B. *Macromo. Symp.* **1995**, *100*, 169.
(18) Park, J.; Kim, H. K.; Son, Y. *Sens. Actuators, B* **2008**, *133*, 244.
(19) Boukai, A. I.; Bunimovich, Y.; Tahir-Kheli, J.; Yu, J.-K.; GoddardIII, W. A.; Heath, J. R. *Nature* **2008**, *451*, 168.
(20) Hicks, L. D.; Dresselhaus, M. S. *Phys. Rev. B* **1993**, *47*, 12727.
(21) Hicks, L. D.; Harman, T. C.; Sun, X.; Dresselhaus, M. S. *Phys. Rev. B* **1996**, *53*, 10493.
(22) Hochbaum, A. I.; Chen, R.; Delgado, R. D.; Liang, W.; Garnett, E. C.; Najarian, M.; Majumdar, A.; Yang, P. *Nature* **2008**, *451*, 163.
(23) Muller, K.; Klapper, M.; Mullen, K. *Macromol. Rapid Commun.* **2006**, *27*, 586.
(24) Zhang, X. Y.; Lee, J. S.; Lee, G. S.; Cha, D. K.; Kim, M. J.; Yang, D. J.; Manohar, S. K. *Macromolecules* **2006**, *39*, 470.
(25) Han, M. G.; Foulger, S. H. *Chem. Commun.* **2005**, *24*, 3092.
(26) Cho, S. I.; Choi, D. H.; Kim, S. H.; Lee, S. B. *Chem. Mater.* **2005**, *17*, 4564.
(27) Zhang, X. Y.; MacDiarmid, A. G.; Manohar, S. K. *Chem. Commun.* **2005**, *42*, 5328.
(28) Huang, J. X.; Virji, S.; Weiller, B. H.; Kaner, R. B. *J. Am. Chem. Soc.* **2003**, *125*, 314.
(29) Su, K.; Nuraje, N.; Zhang, L. Z.; Chu, I. W.; Peetz, R. M.; Matsui, H.; Yang, N. L. *Adv. Mater.* **2007**, *19*, 669.
(30) Kim, D.; Kim, Y.; Choi, K.; Grunlan, J. C.; Yu, C. H. *Acs Nano* **2010**, *4*, 513.
(31) Wang, Y. Y.; Cai, K. F.; Yin, J. L.; An, B. J.; Du, Y.; Yao, X. *J. Nanopart. Res.* DOI: 10.1007/s11051-010-0043-y.
(32) Wang, Y. Y.; Cai, K. F.; Yao, X. *J. Solid State Chem.* **2009**, *182*, 3383.
(33) Yang, Y. J.; Jiang, Y. D.; Xu, J. H.; Yu, J. S. *Polymer* **2007**, *48*, 4459.
(34) Binks, B. P.; Lumsdon, S. O. *Langmuir* **2000**, *16*, 8622.